khazanah informatika

Jurnal Ilmu Komputer dan Informatika

Contact Lens Detection Using Domain Specific BSIF and Discrete Wavelet Transform

Muhamad Ilham Aji Vachroni [1*], Raden Sumiharto [2], Dyah Aruming Tyas [3]
[1,2,3]Departement of Computer Sciences and Electronics
Universitas Gadjah Mada
Yogyakarta, Indonesia
*muhamadilhamajivachroni@ugm.ac.id

Abstract-Iris is one of the reliable biometrics because it has a texture that rich properties and the texture is not changeable lifetime. Iris recognition has drawbacks in the matching process when using contact lenses. Contact lens can changes in the texture of the iris, which can reduce the accuracy of recognition. Therefore, a system is needed to detect contact lenses while someone is detected using contact lens, the system can reject the registration or authentication process. Methods used to detect contact lenses are Domain Specific Binarized Statistical Image Feature (BSIF) and Discrete Wavelet Transform (DWT) for feature extraction. Both methods are fused and modeled using the Support Vector Machine (SVM). Based on the test results, the most optimal kernel is 5x5 12bit. Using the kernel, the accuracy and f1 score obtained 99.1%. In the experiments conducted, this research applies Principal Component Analysis (PCA) to reduce features. However, the role of PCA does not affect the performance of the model. The best model tested with real life data, the Pocophone f1 smartphone and CCTV were used to take pictures of the eyes. The Result 6 experiments wich are 4 without contact lenses and 2 wearing contact lenses, there are only 2 detected correctly. This is because the ability of the images taken from the Poco F1 and CCTV have low resolution.

Keywords: Contact Lens Detection, BSIF, DWT, PCA.

Article info: *submitted October, 14, 2022, revised August, 13, 2023, accepted August, 13, 2023*

1. Introduction

Iris biometric is a reliable authentication system for identification and verification process. This is because iris has texture rich properties feature [1]. Iris also has texture is not changeable lifetime, therefor age does not affect the iris [2]an efficient iris recognition algorithm is presented based on features extracted from Integer Wavelet Transform (IWT. From the experimental results of John Daughman, He stated that out of 9 million people's irises, none of them have the same iris texture [3]. Although iris recognition is a reliable biometric system, iris recognition has a drawback, namely in the matching process when using contact lenses. Contact lens can change the texture of the iris, which can reduce the accuracy of recognition [1]. There are two kinds of contact lenses, including colored contact lens and transparent contact lens. Colored contact lens considered to be the cause of a significant decrease in recognition's accuracy because basically this type of contact lens is designed to change the wearer's appearance, indirectly the design changes the texture pattern of the iris. Meanwhile, transparent contact lens does not significantly reduce recognition accuracy. This is because the type of contact lens is clear or does not contain texture on the contact lens component [4].

Research by [5] and [4] on the effect of contact lens in iris recognition stated that colored contact lens significantly decreased recognition accuracy. Their research, it was stated that at the time of matching between normal and normal, accuracy of 96.76% was obtained, while when matching between normal and transparent the accuracy decrease 0.051% to 96.25%, but when matching between normal and colored the accuracy decrease significantly to 57.03%. Thus, this research will focus on the detection of colored or commonly called contact lens texture.

Binarized Statistical Image Features (BSIF) for feature extraction and Support Vector Machine (SVM) for learning proposed by [6,7] to colored contact lens detection. Using the Clarkson dataset, the two researches obtained an accuracy of 93.3% and 94.3%. Similar research proposed by [8] using Notre Dame Contact Lens Detection (NDCLD'15) dataset stated that BSIF got better result than Local Binary Pattern (LBP) which was 97.65%. Feature extraction Scale Invariant local Descriptors (SID) and SVM with features tuning using Bag-of Features proposed by [1] using IIITD dataset, the research obtained

an accuracy of 93.17%.

Main purpose of this researh is finding the precise texture feature extraction to detect contact lens so when someone is detected using contact lens, the system can reject the registration or authentication process. Binarized Statistical Image Features (BSIF) method has been proven to be accurate in several studies on texture descriptors. This research will use Domain Spesific Binarized Statistical Image Features proposed by [9] which proved to be better than the original BSIF in the iris texture domain. Basic difference from the original BSIF is the kernel used in the descriptor process, Domain Spesific Binarized Statistical Image Features use kernel obtained from iris images learnt by Independent Component Analysis (ICA) with maximizing the statistical independence of the filter responses, while original BSIF use kernel obtained from the natural image patches. This research also will be fusing extraction of these feature with Discrete Wavelet Transform (DWT) which method is proven by research [10,11] that performance better than dual tree complex wavelet packet transform (DTCWPT) and discrete wavelet packet transform (DWPT) for texture analysis Brodatz database. Brodatz database is database that contains 112 kinds of texture from photography albums for artists and designers collected in 1966 in New York. In addition, this research will conduct experiment by applying the reduction feature using Principal Component Analysis (PCA) which has been proven in several fields to speed up computation time and increase accuracy [12].

In order to measures performance of Domain Spesific BSIF and DWT this research using SVM for learning and confusion matrix for validation, which the accuracy and f1 score will be used. Because best kernel of Domain Spesific BSIF isn't found yet, this research will try to find the optimal kernel for texture contact lens detection. The most model optimal will be used to try validation using real life, this research will try using Pochophone f1 that contain infrared camera

2. Methods

a. Acquisition

This research using IIITD dataset wich obtained from lisensi agreement according to established procedures. IIITD is a dataset containing a collection of irises taken using a near infrared sensor. There are two kinds of sensors used, namely Cogent and VistaFA2E. Total number of data is 6570 iris images taken from 202 participants (subjects), each subject contains least 3 iris images [13]iris recognition has gained importance in the biometrics applications and is being used in several large scale nationwide projects. Though iris patterns are unique, they may be affected by external factors such as illumination, camera-eye angle, and sensor interoperability. The presence of contact lens, particularly color cosmetic lens, may also pose a challenge to iris biometrics as it obfuscates the iris patterns and changes the inter and intra-class distributions. This paper presents an in-depth analysis of the effect of contact lens on iris recognition performance. We also present the IIIT-D Contact Lens Iris database with over 6500 images pertaining to 101 subjects. For each subject, images are captured without lens, transparent (prescription. Each subject there are three types of images, namely without contact lenses (none), transparent or soft contact (transparent) lens, and textured or colored contact lens (textured). Images captured using VistaFA2E sensor will be used to create the model. This is because image captured using VistaFA2E better than Cogent, iris image camptured using sensor Cogent almost blur for overall, noise specular light and invariant illumination. Figure 1 shows the difference between VistaFA2E and Cogent sensor results.

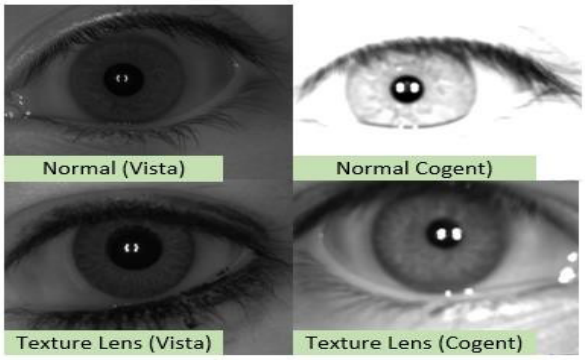

Figure 1. Result sensor Vista and Cogent

The second source of iris data is obtained from the Pocophone f1 smartphone and the Glenz cctv. This data is used to measure how accurate the model is with real live data. Pocophone f1 has an infrared sensor at secondary camera.

b. Segmentation

There are two steps for iris segmentation, first step is pupil localization and scond step is iris localization. In the pupil localization process, fisrt step is global thresholding, This process is most appropriate because basically the color of the pupil has the blackest color between the iris and sclera. Formula (1) shows global thresholding formula.

$$g(x,y) = \begin{cases} 1, & f(x,y) \geq T \\ 0, & f(x,y) < T \end{cases} \quad (1)$$

Where g(x,y) is output from global thresholding, f(x,y) is image input, and T is threshold. The results of global thresholding will be dilated which serves to hit miss transformation. After that apply edge detection using Canny Edge Detection for finding the objects within image, this method proposed by [14]the use of a reliable personal identifier has become a necessity. Using Personal Identification Number (PIN. To perform canny edge detection operations there are 3 stages that must be passed:

1) Noise reduction
There are several methods that can be used for noise reduction, Usually method for reducing noise for this step is a gaussian filter.
2) Gradient Calculation
Detect pixel intensity by calculating the gradient of the image using edge detector operators. The following formula for finding the gradient is as in the Formula 2.

$$|G| = \sqrt{I_x^2 + I_y^2}, \theta(x,y) = \arctan\left(\frac{I_y}{I_x}\right) \quad (2)$$

Where :
G : Magnitude
Θ : Slope
Ix : Horizontal direction
Iy : Vertical direction
3) Non-maximum suppression
This process goes through all the points on the gradient intensity matrix and finds the pixel with the maximum value in the edge direction.

After objects found, Circular Hough Transform (CHT) applied to find circular iris. CHT works maps the edge of the image to the eye resulting from calculating the first derivative of the intensity value. Each point on the edge contributes the circle's radius (r) and center (xc, xy) to the accumulator array. Then, a voting procedure is used to find the largest peak in the resulting accumulator array in the parameter space, which corresponds to the circle that is best defined by the edge point [15]automated identification of individuals based on biometric methods has been a major focus of research and development over the last decade. Biometric recognition analyses unique physiological traits or behavioral characteristics, such as an iris, face, retina, voice, fingerprint, hand geometry, keystrokes or gait. The iris has a complex and unique structure that remains stable over a person's lifetime, features that have led to its increasing interest in its use for biometric recognition. In this study, we proposed a technique incorporating Principal Component Analysis (PCA. Formula (3,4,5) shows CHT formula.

$$H(x_c, y_c, r) \sum_{i=1}^{n} h(x_i, y_i, x_c, y_c, r) \quad (3)$$

$$h = (x_i, y_i, x_c, y_c, r) = \begin{cases} 1, if\ g(x_i, y_i, x_c, y_c, r) = 0 \\ 0, \quad otherwise \end{cases} \quad (4)$$

$$g(x_i, y_i, x_c, y_c, r) = (x_i - x_c)^2 + (y_i - y_c)^2 - r^2 \quad (5)$$

After pupil localized, the next process is iris approximation using Integro-differential Operator (IDO). This method proposed by Jhon Daugman [16]. IDO has been proven to be reliable in iris approximation based on circular pupil [15]. Formula (6) shows the formula IDO.

$$Max(r, x_0, y_0) \left| G_\sigma(r) * \int_{((r,x_0,y_0))} \frac{I(x,y)}{2\pi r} ds \right| \quad (6)$$

The pixel-wise operator looks for the input image, I(x,y), and obtains the fuzzy derivative of the integral over the normalized contour at different radii. The pupillary and limbus boundaries are expected to maximize the derivative of the integral contour, where the intensity value above the circle boundary will make changes to the above. is a smoothing function controlled by σ which smooths the intensity of the image for a more precise search.

c. Feature Extraction

BSIF has been proven more superior than LBP and SID for texture contact lens detection [1,6,8]. This research uses the BSIF method with a specific kernel, namely Domain Specific Binarized Statistical Image Features (DSBSIF) proposed by [9]. Domain Specific BSIF using kernel that learnt from iris domain has been proven more superior than kernal learnt from image natural patch (Original BSIF) for texture iris analysis [9]. BSIF and Domain Specific BSIF have similar works like Local Binay Pattern (LBP) and Local Phase Quantization (LPQ), i.e. perform convolution using a certain filter or kernel and produce a binary value. Binary values in one kernel will be summed, and the result of the sum is the image intensity value. After convoluted, the result of image will be represented by histogram, The histogram will be used as feature extraction. Figure 2 shows illustration how it works.

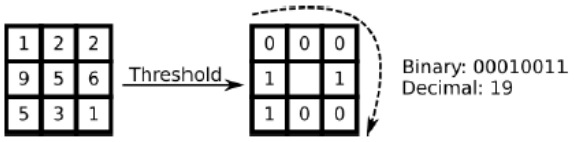

Figure 2. Convert original pixel of image to binary (Gopala K, et all (2018))

Figure 2 left side is kernel and right side is result from *if x >= threshold* then 1, otherwise 0. Kernel used according to result of image patch learnt from domain specific iris and size of kernel. Size of kernel Domain Specific BSIF has two properties namely size l and length n, that is *i* {5,7,9 ,11,13,15,17,19,21,27,33,39} and *n* {5,6,7,8,9,10,11,12}.

The result of the BSIF feature with the domain specific kernel will be fused using DWT, wich has been proven from research [10] that performance DWT beeter than dual tree complex wavelet packet transform (DTCWPT) and discrete wavelet packet transform (DWPT) for texture analysis on the Brodatz database. Similar research proposed by [11] has been proven that DWT more superior than Random Projection and Dense Micro Block Difference for texture analysis from four kinds of texture dataset, that is Brodatz, CUReT, KTH and KTH–TIPS-2a. Figure 3 shows illustration how DWT works.

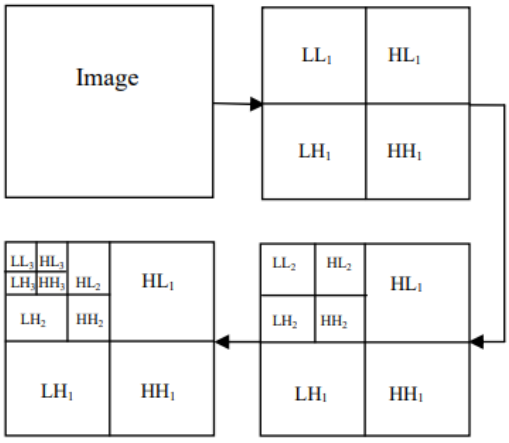

Figure 3. Illustration 3D decomposition of DWT (Source (Kashyap & SINHA, 2012))

In order to obtain feature extraction from 3D level composition DWT is compute Mean (μ) and Standard Deviation (σ) like Formula (7,8).

$$\mu = \frac{1}{N}\sum_{i,j}(Dmi(b_i,b_j)) \quad (7)$$

Where :
N = Total coefision 3D level (10-1 = 9 sub image)
Dmi = Sub image

$$\mu = \frac{1}{N}\sum_{i,j}(Dmi(b_i,b_j))\,. \quad (8)$$

Where :
X = Sub image
X' = Mean
n = Total coefision

d. Feature Fusion

Combining all information (features) which aims to obtain more detailed information [17]. Figure 4 shows illustration of feature fusion.

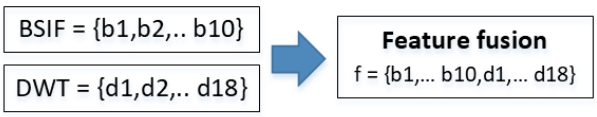

Figure 4. Feature fusion

e. Feature Reduction

Principal Component Analysis is a technique for reducing the dimensions of a data set, improving interpretation without losing important information in a data. PCA does this by creating new variable from look for variance as much as possible [18]. Recently PCA applied for predict energy consumption with data cycles that are always updated [12]. The result of the research stated that using PCA can increase speed up execution time and reduce the Mean Squad Error (MSE) value. This research will compare whether PCA obtain better result or otherwise.

f. Support Vector Machine

This research using Support Vector Machine (SVM) to detect contact lenses. SVM is classifier method that used to look for an optimal separating hyperplane with the maximum margin between the classes. SVM has proven to be able to learn data well. As with the results of the comparison conducted by [19]. The research compare SVM and Convolution Neural Network (CNN) for Hyperspectral image classification on the Chikusei dataset. Using kernel rbf, SVM outperform CNN namely obtain accuracy 98,84%. Meanwhile CNN soft max obtain accuracy 94,01%.

g. Confusion Matrix

Confusion matrix is one of the evaluation methods used to measure accuracy. The confusion matrix composition is in Figure 5 and accuracy formula used is as in Formula 9.

Confusion Matrix		Target			
		Positive	Negative		
Model	Positive	a	b	*Positive Predictive Value*	a/(a+b)
	Negative	c	d	*Negative Predictive Value*	d/(c+d)
		Sensitivity	*Specificity*	**Accuracy** = (a+d)/(a+b+c+d)	
		a/(a+c)	d/(b+d)		

Figure 5. Confusion matrix composition

$$\textit{Accuracy} = (a+d)/(a+b+c+d) \quad (9)$$

Where:
- Accuracy : Proportion of the number of correct predictions
- Positive Predictive Value or Precision : Proportion of positive cases in the predicted outcome
- Negative Predictive Value : Proportion of negative cases in prediction results
- Sensitivity or Recall : Proportion of true positives identified
- Specificity : Proportion of identified true negatives

3. Result

Segmentation using Canny Edge Detection and IDO with a localization process using CHT has been proven to be able to segment well. The following is an illustration of the iris segmentation process as shown in Figure 6.

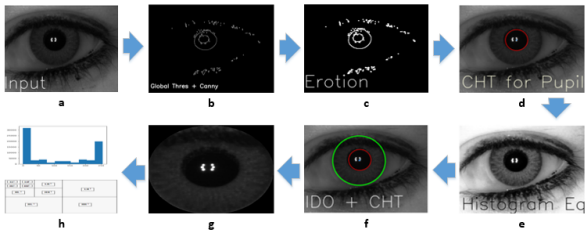

Figure 6. a) input iamge. b) global threshold + canny. c) erotion. d) CHT. e) histogram equalization. f) IDO + CHT. g) segmentation. h) extract features BSIF and DWT

Figure 6.a is input image taken from near infrared camera. 6.b is result of global threshold and canny edge detection. In order to thicken pesudo line from 6.b, erotion applied as 6.c. Furthermore, the localization of the pupil circle is carried out by voting using Circular Hough Transform (CHT). After pupil localization, the next process is image input enhancement using histogram equalization as shown in Figure 6.e and iris approximation using IDO and carried out voting using CHT like as Figure 6.f. After iris localized, the next process is cropping like as Figure 6.g and featurex extraction like as Figure 6.h. While Figure 7 shows result of segmentation.

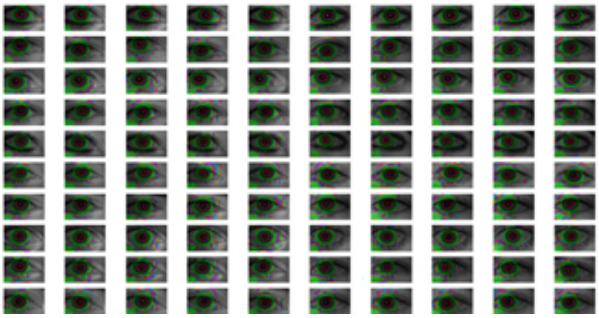

Figure 7. Result segmentation

Figure 7 is result of pupil and iris localization. On the process segmentation this research use default dimension of image, that is 640x480. There are 15 threshold experiments used in the segmentation process, namely 5 to 20. Table 1 shows the experimental result.

Table 1. Threshold experiment

No	Threshold	Fail segmentation	Success segmentaion
1	6	920	1085
2	7	196	1809
3	8	76	1929
4	9	42	1963
5	10	28	1977
6	11	1	2004
7	12	1	2004
8	13	0	2005
9	14	1	2004
10	15	0	2005
11	16	0	2005
12	17	0	2005
13	18	0	2005
14	19	0	2005
15	20	0	2005

The result of experiments that have been carried out state that the threshold with a value 13,15,16,17,18,19, and 20 can segment well.

Experiments carried out 864 times, namely all kernels from Domain Specific BSIF that contains 12 for length (l) and 2 sizes (n), namely 8 bits and 12 bits. Each kernel will be experimented using SVM with 6 parameter combinations, all of them use linear and rbf kernel, and use C values 1,10,and 100 respectively. In the experimental process, single feature and feature fusion applied and each will be compared using PCA. The amount of data used is 2005. 1005 for data with contact lens (CL) and 1000 data without contact lens (no CL). While split of training data and testing data is 70:30. Table 2 shows the best result for each kernel used.

Table 2 contains several columns including the kernel which represents the kernel used in the experiment. While at the BSIF, DWT, and PCA column there are ✔ and ✗ notation. Checklist means to use and a cross means not to use. Feature fusion domain specific BSIF use kernel size 5x5 12bit and DWT get the highest result 99,3%. While the role of PCA in finding the maximum variance has no effect. In the experiments carried out, when the variance is reduced the accuracy will decrease, it means that feature fusion domain specific BSIF and DWT have good information, so SVM is able to learn these features without using PCA.

Table 2. Experiment result

No	Kernel	BSIF	DWT	PCA	SVM		Acc Train	Acc Test	F1 Score
					K	C			
1	5x5 8bit	✔	✔	✗	rbf	10	99,9	98,8	98,
2	5x5 12bit	✔	✔	✗	rbf	100	**100**	**99,1**	**99,14**
3	7x7 8bit	✔	✔	✗	rbf	10	100	98,	98,4
4	7x7 12bit	✔	✔	✗	rbf	10	100	98	97,9
5	9x9 8bit	✔	✔	✗	rbf	10	100	96	95,8
6	9x9 12bit	✔	✔	✗	rbf	100	100	96,6	96,4

No	Kernel	BSIF	DWT	PCA	SVM		Acc Train	Acc Test	F1 Score
					K	C			
7	11x11 8bit	✔	✔	✗	rbf	10	100	96,	95,8
8	11x11 12bit	✔	✔	✗	rbf	10	99,9	97,3	97,7
9	13x13 8bit	✔	✔	✗	rbf	10	99,8	97,1	97
10	13x13 12bit	✔	✔	✗	rbf	10	99,9	97,8	97,7
11	15x15 8bit	✔	✔	✗	rbf	10	99,7	95,8	95,7
12	15x15 12bit	✔	✔	✗	rbf	10	99,9	97,1	97
13	17x17 8bit	✔	✔	✗	rbf	10	99,7	96,8	96,7
14	17x17 12bit	✔	✔	✗	rbf	100	100	97,3	97,2
15	19x19 8bit	✔	✔	✔	rbf	10	99,8	96,	95,8
16	19x19 12bit	✔	✔	✗	rbf	10	99,9	96,1	96
17	21x21 8bit	✔	✔	✗	rbf	100	100	97,	96,9
18	21x21 12bit	✔	✔	✗	rbf	10	99,6	97,1	97
19	27x27 8bit	✔	✔	✗	rbf	100	100	96,1	96
20	27x27 12bit	✔	✔	✗	rbf	100	100	96,5	96,4
21	33x33 8bit	✔	✔	✗	rbf	100	100	95,8	95,7
22	33x33 12bit	✔	✔	✗	rbf	100	100	95,8	96,6
23	39x39 8bit	✔	✔	✗	rbf	100	100	96,3	96,2
24	39x39 12bit	✔	✔	✗	rbf	100	100	95	94,9

4. Discussion

When compared with previous research, the proposed method is superior to previous research. The following table 3 compares the proposed method with the previous method.

The best model from IIITD dataset using VistaFA2E sensor then tested with real life data captured from pocophone f1 smartphone and cctv G-lenz. Figure 8 shows the test result.

Figure 8 is an example of the result of real life images and dataset images. The top image is input, the middle image is a segmented image, and the bottom image is the BSIF descriptor image. Figure 9 is a histogram representing the features of the BSIF descriptor.

Table 3. Comparison of results with previously

No	Author	Method	Dataset	Accuracy
1	Kulkarni P et al., (2019)	Weber Local Descriptor (WLD) and SVM	IIITD	97,5 %
2	Dronk y et al., (2021)	BSIF and SVM	Clarkson 2013	93,3%

No	Author	Method	Dataset	Accuracy
3	Gragnaniello et al., (2016)	Scale-invariant local descriptors (SID) and SVM + Bag-of- features	IIITD	93,1%
4	Doyle & Bowy er., (2015)	BSIF and Random Forest	NDCLD 2015	84%
5	Yadav et al., (2013)	LBP and SVM	IIITD	80%
6	**Proposed method**	**Domain Specific BSIF + DWT and SVM**	**IIITD**	**99,1%**

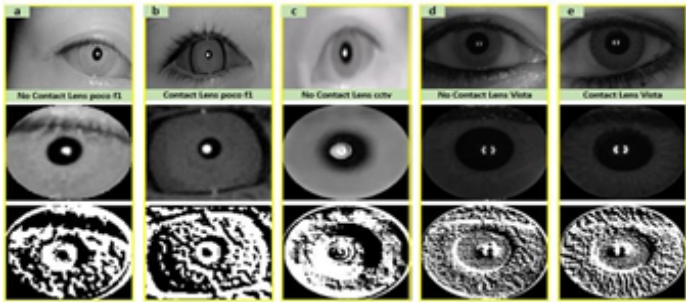

Figure 8. a) no CL captured poco f1. b) using CL captured by poco f1. c) no CL captured cctv. d) no CL captured Vista. e) using CL captured by Vista

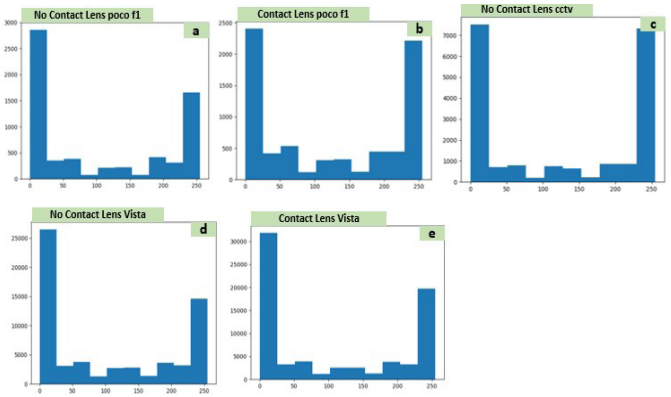

Figure 9. a) histogram no CL captured poco f1. b) histogram using CL captured by poco f1. c) histogram no CL captured cctv. d) histogram no CL captured Vista. e) histogram using CL captured by Vista

Table 4. Distance feature extraction real life and dataset for darkest pixel and brightest pixel histogram

No	Data	Dist CL (darkest)	Dist CL (brightest)	Dist no CL (darkest)	Dist no CL (brightest)
1	No CL poco f1	**3470,67**	**1306,60**	3592,19	1631,39
2	CL poco f1	**49578,28**	**77336,84**	49699,80	77661,63
3	No CL cctv	**1380,47**	**4517,57**	1501,99	4842,36
4	No CL Vista	1502,40	1646,97	**1380,88**	**1322,19**
5	CL Vista	**2487,80**	**2358,78**	2609,32	2683,56

Table 5. Distance feature extraction real life and dataset for all pixel histogram

No	Data	Dist CL	Dist no CL
1	No CL poco f1	**5522,58**	5742,72
2	CL poco f1	**74063,58**	74231,62
3	No CL cctv	**3660,21**	3831,04
4	No CL Vista	2304,29	**2036,64**
5	CL Vista	**3541,19**	3713,19

The result of 6 experiments with the composition of each 2 images as in Figure 8 of them 4 without wearing contact lenses and 2 wearing contact lenses, only 2 have been detected correctly. All experimental result were detected using contact lens. If seen visually Figure 8.a and Figure 8.b produce low dimension images. Thus, when transformed into texture analysis, the pixel intensity tend to be dominated by dark as in Figures 9.a and 9.b. Beside that, if seen visually Figures 8.d and 8.e the result of the capture on the dataset used, Iris with contact lens contains a denser texture density than without using contact lenses. Thus, the pixel intensity tends to be dominated by dark as in figure 9.e. Beside that the capture from CCTV is too blurry, although visually the density of the texture is not like the results of the caputure pocophone f1, but the pixel intensity tends to be dominated by dark too. Thus, this research states that all real life results are detected using contact lenses becauseof low dimension of the image, thus dark pixels dominate, which means the same as the average feature extraction on the dataset using contact lenses. This statement is based on the analysis of the shortest distance between real life data and datasets, both contact lens and without contact lens for the darkest pixels, brightest, and all pixels in the histogram. In order to calculate distance this research using euclidience distance. The result of the analysis of the distance between real life and dataset are shown in Tables 4 and 5.

Table 4 and 5 shows the result of the analysis of the distance between real life data and datasets based on histograms. Feature representation for real life data will be calculated using Euclidean distance with the average feature representation in the dataset. The results obtained are in accordance with the previous statement that all real life results are detected using contact lenses because of the low dimension in the image, so dark pixels dominate, which means the same as the average feature extraction on the dataset using contact lens.

5. Conclusion

Iris is one of the reliable biometrics because it has a texture that rich properties and the texture is not changeable lifetime. This riches of features is used to recognize the identity of a person with a machine learning approach. Presence of textured or colored contact lens in the eye affect in exchange of iris texture, thereby it could reduce the accuracy of the iris recognition system. Thus, a preprocess recognition system is needed, which aims when someone is detected using a contact lens, the system can reject the registration or authentication process. Domain Specific BSIF with kernel size 5x5 12bit and DWT get the highest result compared to other kernels able to be applied well to the IIITD dataset. Using the kernel, the accuracy and f1 score obtained 99.1%. The role of PCA has no effect on accuracy, when lower variance used so does it has lower accuracy. It means that all the features in Domain Specific BSIF and DWT contain good information, therefore SVM able to learn data well.

The best model testing is applied to real life, namely the iris captured from the Pocophone f1 smartphone and the G-lenz cctv. The Result 6 experiments wich are 4 without contact lenses and 2 wearing contact lenses, there are only 2 detected correctly. There are several reasons why it fails to be applied in real life. First, it is because of low dimension so that when it is transformed into texture analysis, pixel intensity tends to be dominated by dark. Second, textures on the iris can't be captured well so the detail of textures is hardly to visible. Third, the image is the result of the cctv blur so the texture doesn't look well.

Acknowledgement

Thank you to Image Analysis And Biometrics Lab IIT Jodpur for giving permission to use the iris dataset in this research.

Reference

[1] D. Gragnaniello, G. Poggi, C. Sansone, and L. Verdoliva, "Using iris and sclera for detection and classification of contact lenses," *Pattern Recognit. Lett.*, vol. 82, pp. 251–257, Oct. 2016, doi: 10.1016/j.patrec.2015.10.009.

[2] G. Singh, R. K. Singh, R. Saha, and N. Agarwal, "IWT Based Iris Recognition for Image Authentication," *Procedia Comput. Sci.*, vol. 171, no. 2019, pp. 1868–1876, 2020, doi: 10.1016/j.procs.2020.04.200.

[3] H. Y. Sun Yangqing, *Image Preprocessing of Iris Recognition*. IEEE, 2018.

[4] D. Yadav, N. Kohli, J. S. Doyle, R. Singh, M. Vatsa, and K. W. Bowyer, "Unraveling the Effect of Textured Contact Lenses on Iris Recognition," 2013. [Online]. Available: http://www3.nd.edu/.

[5] A. Nigam, B. Kumar, and P. Gupta, "Robust Contact Lens Detection Using Local Phase Quantization and Binary Gabor Pattern," *Lect. Notes Comput. Sci. (including Subser. Lect. Notes Artif. Intell. Lect. Notes Bioinformatics)*, vol. 9256, pp. 702–714, 2015, doi: 10.1007/978-3-319-23192-1.

[6] M. R. Dronky, W. Khalifa, and M. Roushdy, "Using residual images with BSIF for iris liveness detection," *Expert Syst. Appl.*, vol. 182, Nov. 2021, doi: 10.1016/j.eswa.2021.115266.

[7] M. R. Dronky, W. Khalifa, and M. Roushdy, "Impact of segmentation on iris liveness detection," 2019.

[8] J. S. Doyle and K. W. Bowyer, "Robust Detection of Textured Contact Lenses in Iris Recognition Using BSIF," *IEEE Access*, vol. 3, pp. 1672–1683, 2015, doi: 10.1109/ACCESS.2015.2477470.

[9] A. Czajka, D. Moreira, K. W. Bowyer, and P. J. Flynn, "Domain-specific human-inspired

binarized statistical image features for Iris recognition," *Proc. - 2019 IEEE Winter Conf. Appl. Comput. Vision, WACV 2019*, pp. 959–967, 2019, doi: 10.1109/WACV.2019.00107.

[10] S. Dhanya and V. S. Kumari Roshni, "Comparison of various texture classification methods using multiresolution analysis and linear regression modeling," *Springerplus*, vol. 5, no. 1, pp. 1–18, 2016, doi: 10.1186/s40064-015-1631-1.

[11] K. Gopala Krishnan and P. T. Vanathi, "An efficient texture classification algorithm using integrated Discrete Wavelet Transform and local binary pattern features," *Cogn. Syst. Res.*, vol. 52, pp. 267–274, 2018, doi: 10.1016/j.cogsys.2018.07.015.

[12] T. Parhizkar, E. Rafieipour, and A. Parhizkar, "Evaluation and improvement of energy consumption prediction models using principal component analysis based feature reduction," *J. Clean. Prod.*, vol. 279, 2021, doi: 10.1016/j.jclepro.2020.123866.

[13] N. Kohli, D. Yadav, M. Vatsa, and R. Singh, "Revisiting iris recognition with color cosmetic contact lenses," *Proc. - 2013 Int. Conf. Biometrics, ICB 2013*, vol. 1, 2013, doi: 10.1109/ICB.2013.6613021.

[14] H. A. Biu, R. Husain, and A. S. Magaji, "AN ENHANCED IRIS RECOGNITION AND AUTHENTICATION SYSTEM USING ENERGY MEASURE," *Sci. World J.*, vol. 13, no. 1, 2018, [Online]. Available: www.scienceworldjournal.org.

[15] H. K. Rana, M. S. Azam, M. R. Akhtar, J. M. W. Quinn, and M. A. Moni, "A fast iris recognition system through optimum feature extraction," *PeerJ Comput. Sci.*, vol. 2019, no. 4, pp. 1–13, 2019, doi: 10.7717/peerj-cs.184.

[16] J. Daugman, "How Iris Recognition Works," *IEEE Trans. Circuits Syst. Video Technol.*, vol. 14, no. 1, pp. 21–30, Jan. 2004, doi: 10.1109/TCSVT.2003.818350.

[17] B. Attallah, A. Serir, Y. Chahir, and A. Boudjelal, "Histogram of gradient and binarized statistical image features of wavelet subband-based palmprint features extraction," *J. Electron. Imaging*, vol. 26, no. 06, p. 1, 2017, doi: 10.1117/1.jei.26.6.063006.

[18] I. T. Jollife and J. Cadima, "Principal component analysis: A review and recent developments," *Philos. Trans. R. Soc. A Math. Phys. Eng. Sci.*, vol. 374, no. 2065, 2016, doi: 10.1098/rsta.2015.0202.

[19] H. Hasan, H. Z. M. Shafri, and M. Habshi, "A Comparison between Support Vector Machine (SVM) and Convolutional Neural Network (CNN) Models for Hyperspectral Image Classification," *IOP Conf. Ser. Earth Environ. Sci.*, vol. 357, no. 1, 2019, doi: 10.1088/1755-1315/357/1/012035.